HHS Public Access

Author manuscript

Mucosal Immunol. Author manuscript; available in PMC 2024 February 05.

Published in final edited form as:

Mucosal Immunol. 2023 December ; 16(6): 788–800. doi:10.1016/j.mucimm.2023.08.003.

LAIR-1 limits macrophage activation in acute inflammatory lung injury

Doumet Georges Helou[1,2], **Christine Quach**[1], **Benjamin P. Hurrell**[1], **Xin Li**[1], **Meng Li**[3], **Amitis Akbari**[1], **Stephen Shen**[1], **Pedram Shafiei-Jahani**[1], **Omid Akbari**[1,✉]

[1]Department of Molecular Microbiology and Immunology, Keck School of Medicine, University of Southern California, Los Angeles, California, USA.

[2]Université Paris Cité, UFR de Médecine, Inserm U1152, Physiopathologie et épidémiologie des maladies respiratoires, Paris, France.

[3]USC Libraries Bioinformatics Service, University of Southern California, Los Angeles, California, USA.

Abstract

Acute lung injury (ALI) and acute respiratory distress syndrome (ARDS) are serious health problems that manifest as acute respiratory failure in response to different conditions, including viral respiratory infections. Recently, the inhibitory properties of leukocyte-associated immunoglobulin-like receptor-1 (LAIR-1) were demonstrated in allergic and viral airway inflammation. In this study, we investigate the implication of LAIR-1 in ALI/ARDS and explore the underlying mechanisms. Polyinosinic:polycytidylic acid, a synthetic analog of double-stranded RNA, was used to mimic acute inflammation in viral infections. We demonstrate that LAIR-1 is predominantly expressed on macrophages and regulates their recruitment to the lungs as well as their activation in response to polyinosinic:polycytidylic acid. Interestingly, LAIR-1 deficiency increases neutrophil recruitment as well as lung resistance and permeability. In particular, we highlight the capacity of LAIR-1 to regulate the secretion of CXCL10, considered a key marker of macrophage overactivation in acute lung inflammation. We also reveal in COVID-19-induced lung inflammation that *LAIR1* is upregulated on lung macrophages in correlation with relevant immune regulatory genes. Altogether, our findings demonstrate the implication of LAIR-1 in the pathogenesis of ALI/ARDS by means of the regulation of macrophages, thereby providing the basis of a novel therapeutic target.

✉ akbari@usc.edu .

AUTHOR CONTRIBUTIONS

D.G.H. designed and performed experiments, analyzed results, and wrote the manuscript. C.Q., B.P.H., and S.S. contributed to the interpretation of the data and helped perform experiments. M.L., X.L., and A.A. provided expertise for transcriptomic analysis and reviewed the manuscript. P.S-J. provided animal husbandry for experiments. O.A. supervised, designed the experiments, interpreted the data, and critically reviewed the manuscript.

DECLARATIONS OF COMPETING INTERESTS

The authors have no competing interests to declare.

APPENDIX A. SUPPLEMENTARY DATA

Supplementary data to this article can be found online at https://doi.org/10.1016/j.mucimm.2023.08.003.

INTRODUCTION

Acute lung injury (ALI) and acute respiratory distress syndrome (ARDS), the severe form of ALI, are the leading causes of progressive respiratory failure in critically ill patients. Severe hypoxemia in ARDS mainly results from acute pulmonary inflammation leading to alveolar edema and decreased lung compliance[1–3]. Disease severity correlates with the intensity of uncontrolled cytokine storms and, therefore, with high mortality rates reaching up to 50% of patients[4,5]. The main causes of ALI/ARDS are sepsis, severe chest injury, toxic chemical inhalation, and viral pneumonia[2,6,7]. In particular, ARDS was the most serious and lethal complication during the outbreak of coronavirus disease 2019 (COVID-19), with a mortality rate as high as 39%[8–10]. Tackling this fatal complication necessitates a thorough understanding of the immune mechanisms that dictate ALI/ARDS poor prognosis. For that, different mouse models were developed to reproduce the main features of human lung injury[11,12]. Lung stimulation with Polyinosinic-polycytidylic acid (Poly[I:C]), a synthetic analog of viral double-stranded RNA (dsRNA), has the potential to mimic acute inflammatory responses to viral infection and is commonly used in mouse models of ARDS[13–16].

Macrophages are heterogeneous and highly plastic immune cells that are able to shape acute inflammation through diverse immunomodulatory functions. Notably, during the acute phase of ARDS, known as the exudative phase, recruited alveolar macrophages (AMs) acquire a classically activated phenotype (M1) responsible for the release of several growth factors and proinflammatory cytokines, including CXCL1, CXCL2, CXCL10, CCL2, and tumor necrosis factor-α. The resulting chemotactic microenvironment promotes lung injury through the recruitment of neutrophils and inflammatory monocytes/macrophages to the lung. In parallel, interstitial macrophages are further implicated in pathogen and apoptotic cell clearance, tissue repair, antigen presentation, and modulation of other immune cells during the rehabilitation phase of ARDS[17–19].

Like other immune cells, macrophages dispose of multiple regulatory mechanisms that orchestrate their activation and polarization in acute inflammation. It has become increasingly apparent that macrophages can express a variety of regulatory immune receptors belonging to the immune checkpoint family. Recent studies have documented the expression of inhibitory immune checkpoints such as programmed death-1, V-domain immunoglobulin suppressor of T-cell activation, and T-cell immunoglobulin and mucin domain 3, on macrophages in infectious and inflammatory diseases[20]. Moreover, the inhibitory functions of the novel immune checkpoint target leukocyte-associated immunoglobulin-like receptor-1 (LAIR-1), were described in monocytes and macrophages[21–24].

LAIR-1 is a transmembrane glycoprotein inhibitory receptor that is widely expressed on different immune populations with varying expression levels[25–27]. While antigen-presenting cells can express LAIR-1 at the basal state, neutrophils and type-2 innate lymphoid cells only display expression following their activation[28,29]. LAIR-1 is mainly known as a collagen receptor and can consequently interact with other proteins that contain collagen-like repeating sequences, such as C1q and Colec12[24,25,30]. The engagement of

LAIR-1 is intimately tied to immunoreceptor tyrosine-based inhibitory motifs downstream signaling and the recruitment of Src homology region 2 domain-containing phosphatase-1, therefore leading to negative regulatory effects on immune cells, as demonstrated in many inflammatory contexts, including rheumatoid arthritis, systemic lupus erythematosus, and recently in allergic asthma[28,31–33].

In this study, we demonstrated that LAIR-1 deficiency results in increased macrophage activation and recruitment to the lungs. Furthermore, LAIR-1 limits the production of key chemokines in the lungs and reduces lung permeability in ALI/ARDS model. Interestingly, mouse results correlate with transcriptomic data from patient lungs with COVID-19. Therefore, LAIR-1 participates in the regulation of ALI/ARDS and could represent a novel therapeutic target against fatal respiratory complications.

RESULTS

Macrophages display the highest expression of LAIR-1 in ARDS mouse model

We first investigated the role of LAIR-1 in an established model of Poly(I:C)-induced acute lung inflammation, in which Poly(I:C) is used as a surrogate for viral dsRNA to reproduce the inflammatory aspects of ALI/ARDS in viral pneumonia. Mice received 3 intranasal doses of Poly(I:C) on 3 consecutive days and were euthanized on day 4 to collect lungs for immune phenotyping (Fig. 1A). Poly(I:C) stimulation significantly upregulates the expression of LAIR-1 as well as the percentage of LAIR-1$^+$ cells from total pulmonary CD45$^+$ cells (Fig. 1B–D). Interestingly, the majority of LAIR-1$^+$ cells in both control (phosphate buffer saline [PBS]) and Poly(I:C) groups were represented by CD64$^+$ pulmonary cells that include different macrophage subsets in the lungs (Fig. 1E). Then the gating strategy described in Fig. 1F was used to further assess the expression of LAIR-1 on main myeloid immune cells in response to Poly(I:C). As expected, CD11b^{high} CD64$^+$ macrophage subset, representing interstitial macrophages and recruited monocytes/macrophages[34], display the highest expression of LAIR-1 in comparison with neutrophils, patrolling monocytes, AM, total dendritic cells (DCs), and plasmacytoid DCs (pDCs) (Fig. 1G). This suggests that LAIR-1 can play a role in ALI/ARDS by means of the regulation of pulmonary macrophages.

LAIR-1 downmodulates cytokine-related signaling pathways in macrophages

To evaluate the implication of LAIR-1 in the transcriptional activity of lung macrophages in response to Poly(I:C) stimulation, we introduced here the LAIR-1 knockout (KO) mouse on the C57BL/6J background. Wild-type (WT) and LAIR-1 KO mice received Poly(I:C) or PBS intranasally for 3 days, and the CD11b^{high} CD64$^+$ cell subset that previously showed the highest expression of LAIR-1 was fluorescence-activated cell sorting (FACS)-sorted on day 4 (Supplementary Fig. 1). Using RNA-sequencing analysis, we demonstrated that LAIR-1 deficiency significantly modulates the transcriptomic profile of activated macrophages and results in 1580 significantly modulated genes (counts of <20, $p < 0.05$) (Fig. 2A). To better explore the underlying signaling, we performed pathway analysis using gene-level statistics to compute pathway-level scores. In line with previous studies[28,35], the phosphoinositide 3-kinase (PI3K)/protein kinase B (AKT) pathway was

highly upregulated in LAIR-1 KO compared to WT macrophages, along with pathogen-induced cytokine storm pathways. Other inflammatory axes including p38 mitogen-activated protein kinase, Signal transducer and activator of transcription 3, Inducible nitric oxide synthase, and toll-like receptor signaling pathways were significantly upregulated in LAIR-1 KO macrophages. In parallel, regulatory pathways including hepatocyte growth factor, autophagy, and Peroxisome proliferator-activated receptor signaling were significantly downmodulated (Fig. 2B). The nuclear factor-κB (NF-kB) pathway was also explored since it can connect PI3K/AKT and cytokine storm pathways[36,37]. A list of key genes belonging to the NF-kB pathway such as *Myd88*, *Cd40*, and *Rel* showed differential upregulation in LAIR-1 KO macrophages, as represented in the heatmap (Fig. 2C). In the same context, the majority of genes from pathogen-induced cytokine storm pathways, including *Il1b*, *Ccl2*, *Cxcl1*, *Cxcl10,* and *Il12b* were significantly upregulated in the absence of LAIR-1 (Fig. 2D). Although LAIR-1 deficiency promoted the upregulation of several genes associated with inflammatory macrophage phenotype (M1), we could not measure a clear effect of LAIR-1 on the M1/M2 polarization at the transcriptomic level (Fig. 2E). Taken together, these data indicate that LAIR-1 negatively regulates relevant inflammatory pathways in Poly(I:C)-activated macrophages during acute lung inflammation.

LAIR-1 deficiency potentiates macrophage recruitment and activation in response to Poly(I:C)

Given the effect of LAIR-1 deficiency on inflammatory gene activity, we further wanted to confirm LAIR-1 implication in macrophage recruitment and activation in the lungs. Macrophages constitute a very heterogeneous population; therefore, we wanted to check first the effect of LAIR-1 deficiency on the distribution of the main subsets of $CD11b^{high}$ $CD64^{+}$ macrophages according to the expression of MHCII and Ly6C markers. In naive mice lungs, the predominant subset was $MHCII^{+}$ $Ly6C^{\bullet}$, representing therefore interstitial macrophages[34]. In parallel, Poly(I:C) stimulation induced a remarkable rearrangement in the distribution of macrophage subsets mainly characterized by the emergence of inflammatory $Ly6C^{+}$ cells that do or do not express the MHCII marker (Fig. 3A). Nevertheless, LAIR-1 deficiency did not significantly affect the distribution of these subsets in response to Poly(I:C) (Fig. 3B). We then evaluated the recruitment of $CD11b^{high}$ $CD64^{+}$ macrophages in the lungs, as well as the number of monocytes, total DCs, and pDCs. No significant differences were observed between WT and LAIR-1 KO control mice, indicating that LAIR-1 does not affect the homeostasis of these populations in the lungs. In response to Poly(I: C), only the number of macrophages was increased and showed a significant upregulation in LAIR-1 KO mice as compared to WT mice, while the lack of LAIR-1 did not affect the number of monocytes, total DCs, and pDCs (Figs. 3C–E and Supplementary Fig. 2). Since both mice genotypes have a similar distribution of macrophage subsets, we sorted total $CD11b^{high}$ $CD64^{+}$ cells from Poly(I:C)-stimulated lungs to compare cytokine production in culture after 24 hours (Fig. 3F). CXCL10 was remarkably highly secreted in culture and was significantly upregulated in LAIR-1 KO as compared to WT macrophages (Fig. 3G). Moreover, CCL5 and CCL2 were higher in LAIR-1 KO macrophage culture (Figs. 3H and 3I). In parallel, functional assays did not show a significant effect of LAIR-1 deficiency on glucose uptake suggesting that the increased activation of LAIR-1 KO macrophages does not or minorly affect their glycolytic demand (Supplementary Fig.

3). Moreover, WT and KO macrophages showed a similar capacity to phagocyte zymosan bioparticles, suggesting that LAIR-1 is not involved in the regulation of phagocytosis in Poly (I:C)-induced acute lung inflammation (Supplementary Fig. 4). This is in line with previous studies showing that LAIR-1 does not affect the phagocytic index of bone marrow-derived macrophages even in the presence of the physiological ligand C1q[38]. Altogether, these results indicate that LAIR-1 limits macrophage recruitment and cytokine production in acute lung inflammation.

LAIR-1 deficiency enhances lung resistance and neutrophil recruitment to alveoli in response to Poly(I:C)

Airflow resistance is one among other features of ALI/ARDS in animal models[39]. More importantly, neutrophil infiltration and capillary-alveolar permeability are the major hallmarks of ARDS. We, therefore, investigated the effect of LAIR-1 deficiency on these key features in Poly(I:C)-induced acute lung inflammation. WT and LAIR-1 KO mice received intranasal doses of Poly(I:C) on 3 consecutive days. On day 4, lung function was assessed before euthanasia by direct measurement of lung resistance in anesthetized tracheostomized mice using the FinePointe RC system (Buxco Research Systems) (Fig. 4A). As expected, Poly(I:C) stimulation induced airway hyperreactivity in response to increasing concentrations of methacholine as compared to PBS control mice. Moreover, LAIR-1 KO mice displayed higher lung resistance in response to methacholine doses as compared to WT, suggesting an exacerbated alteration of lung respiratory functions (Fig. 4B). Additionally, immune $CD45^+$ cells showed higher recruitment to the airway lumen as revealed by flow cytometry analysis in the bronchoalveolar lavage (BAL) (Figs. 4C and 4D). This is mainly due to the increased recruitment of neutrophils, which constitute the most frequent population in Poly(I:C)-treated mice (Fig. 4E). The number of AM in the BAL was not affected by the genotype and/or the inflammation, as shown in a recent study[24] (Fig. 4F). However, T-cell count in the BAL increased in response to Poly(I:C) but was not significantly different when comparing WT and LAIR-1 KO mice. To compare lung permeability, the fluorescein isothiocyanate (FITC)-labeled dextran assay was performed via the intranasal route. Poly(I:C) stimulation induced a remarkable leakage of the FITC-Dextran from the alveolar space to the blood, confirming the relevance of this mouse model to study ALI/ARDS. In line with our previous data, LAIR-1 KO mice displayed significantly higher levels of FITC in the plasma as compared to WT mice, revealing increased lung permeability (Fig. 4H). Despite the increased protein leakage, LAIR-1 KO mice still display a higher total protein concentration in the BAL, suggesting a more potent lung inflammation as compared to WT mice (Fig. 4I). Altogether, these results suggest that LAIR-1 contributes to the downregulation of lung resistance, permeability, and inflammation in ALI/ARDS.

LAIR-1 reduces the Poly(I:C)-induced cytokine storm in ALI/ARDS

Excess production of chemokines by lung macrophages results in an exacerbated recruitment of inflammatory cells in ARDS. To identify the most relevant macrophage-secreted chemokines in ALI/ARDS, we established a list of genes according to their expression levels in our Poly(I:C) mouse model. In particular, the gene coding for CXCL10 displayed the highest expression in lung macrophages from Poly(I:C)-treated mice, followed by those coding for CCL9, CXCL16, CXCL2, CCL4, CCL2, and CCL3 (Fig. 5A). In

parallel, we quantified the protein levels in the BAL of different relevant chemokines. The level of CXCL10 was extremely high in line with the measured gene and protein expression in macrophages and was significantly higher in the BAL from LAIR-1 KO mice as compared to WT mice (Fig. 5B). Similarly, Poly(I:C)-stimulated mice displayed considerable levels of CCL2, that were higher in LAIR-1 KO mice (Fig. 5C). Other cytokines that are less specific to macrophages such as tumor necrosis factor-α, CCL5, and CXCL1 were also upregulated in the BAL of LAIR-1 KO mice (Figs. 5D–F). Since Poly(I:C) stimulation can mimic to some extent the products of viral infections, we compared the levels of cytokines from the interferon family and detected significant differences in IFN-α and IFN-γ but not in IFN-β (Figs. 5G–I). Taken together, these data confirm that the modulation of cytokine secretion via LAIR-1 is a key regulatory mechanism in ALI/ARDS.

The COVID-19-induced lung injury is associated with *LAIR1* upregulation in pulmonary macrophages

The mechanisms of lung injury in COVID-19 infection are closely related to inflammatory cell-mediated damage associated with massive cytokine production. In this context, many studies have implemented murine SARS-CoV-2 ALI/ARDS models using Poly(I: C) to mimic the effect of viral RNA[40,41]. Using 3 publicly available studies, we aimed to assess the expression of *LAIR1* in COVID-19-induced lung injury. The first study was performed on nuclei from 19 COVID-19 decedent frozen lungs and 7 control patients with short postmortem interval autopsies[42]. Uniform manifold approximation and projection clustering on total cells from control and patients with COVID-19 indicate that myeloid cells display the highest expression of *LAIR1* gene, while the expression stays relatively weak on other immune cells, including T/B lymphocytes and mast cells (Fig. 6A). The breakdown of myeloid cell populations reveals that AM significantly upregulates the expression of *LAIR1* in patients with COVID-19, as well as monocyte-derived macrophages upon entering the lung tissue (Fig. 6B). To confirm our first observations, we evaluated LAIR-1 induction in another single-cell RNA sequencing (scRNA-seq) study performed on BAL from healthy, mild, and severe patients with COVID-19[43]. Filtering and cell type annotation were applied according to the original study (GSE145926), and each color-coded cluster represents one cell type. *LAIR1*$^{-}$cells are in dim color. The t-distributed stochastic neighbor embedding plots reveal that *LAIR1* expression is significantly induced on macrophages (orange dots) in mild and severe patients with COVID-19 (Figs. 6C–F). The Pearson correlation coefficient was calculated to establish a list of the top 100 correlatively expressed genes in relation with *LAIR1* expression in lung macrophages (Fig. 6G). Given that immune cells do upregulate the expression of inhibitory receptors to counteract the activity of activatory pathways[44], simultaneous induction of inhibitory and activatory pathways is expected. Although very heterogeneous, this list highlights significant correlations between *LAIR1* and other inhibitory genes, including *LYN*, *LILRB4*, *IL10RA*, *SIRPA*, *ANXA4*, and *TGFB1*. We also established a correlation between the expression of LAIR1 and the different markers that were identified in our mouse studies. The heatmap on the right shows that, similar to the mouse ALI/ARDS model, *CCL2*, *CCL3*, *CCL4*, *CCL7,* and *CXCL10* are among the most induced genes coding for chemokines in macrophages from severe patients with COVID-19 compared to healthy controls. This demonstrates that the Poly(I:C)-induced

lung inflammation in mice can mimic to a great extent the chemokine environment of COVID-19 infection. To further investigate the link between *LAIR1* induction in lung macrophages and COVID-19 severity, we included a third scRNA-seq study analyzing airway samples from patients with severe COVID-19 infection[45]. In the listed 4 patients, a strong and remarkable correlation was observed between the expression of *LAIR1* in macrophages and several genes including *TGFB1, CXCL16, CCL2, and CCL3* (Fig. 6H). This confirms the implication of LAIR-1 in the tug-of-war between activatory and inhibitory pathways in this context of lung inflammation. To connect all 3 scRNA-seq datasets used in this study, a Venn diagram was created with the top 500 correlative genes. Interestingly, 73 genes represent the overall overlap between the 3 studies. Moreover, 6 genes implicated in inhibitory axes, including *HLA-E*, *LAPTM5*, *MAFB*, *CD68*, *SIRPA*, and *HAVCR2*, do overlap between the 3 studies, providing therefore new LAIR-1-related immune targets.

DISCUSSION

This study relies on a robust mouse model of ALI/ARDS sharing relevant features to ARDS pathogenesis and fulfilling the requirements set by the 2011 American Thoracic Society Workshop. Using this model, we demonstrated that LAIR-1 is principally expressed on macrophages and modulates inflammatory pathways that mediate cytokine secretion. Furthermore, we showed that LAIR-1 downregulates several aspects of ALI/ARDS and confirmed the negative effect of LAIR-1 on the acute release of pro-inflammatory mediators.

A recent study by Kumawat et al. has reported the capacity of LAIR-1 to limit neutrophil and lymphocyte recruitment in respiratory syncytial virus infection[46]. To understand whether LAIR-1 represents a simple activation biomarker or an efficient regulatory mechanism in viral-induced lung injury, a Poly(I:C) acute inflammation model was established in mice. Recognition of Poly(I:C) dsRNA as a viral product occurs mainly via the toll-like receptor 3 and mediates a sustained activation of the innate immune system marked by pro-inflammatory cytokine production. Interestingly, LAIR-1 is highly expressed on macrophages among other myeloid cells in our Poly(I:C)-induced acute inflammation model and significantly downmodulates pathogen-induced cytokine storm pathways with other related pathways, including PI3K/AKT, p38 mitogen-activated protein kinase, and NF-kB, at the transcription level. Our previous study showed that LAIR-1 mainly affects NF-kB as well as the PI3K/AKT pathway via the recruitment of the phosphatase Src homology region 2 domain-containing phosphatase-1 in type-2 innate lymphoid cells. Consistently, several studies have reported the inhibitory function of LAIR-1 in monocytes and macrophages[21,23]. Taken together, LAIR-1 is suggested here as a negative regulator of macrophage inflammatory phenotype in the context of ALI/ARDS.

Resident macrophages are among the first cells to sense damage-associated molecular patterns and to secrete mediators for inflammatory cell recruitment during the exudative phase of ALI/ARDS. Following the early and massive lung infiltration by neutrophils, recruited monocytes join resident macrophages to orchestrate the neutrophil-mediated lung injury. Poly(I:C) stimulation in our mouse model remarkably induced the recruitment of inflammatory cells expressing both Ly6C and CD64 and representing an intermediate monocyte/macrophage inflammatory phenotype[34]. This is associated with high levels

of CXCL10 in the BAL, followed by CCL5 and CCL2, all known to be implicated in neutrophil and monocyte recruitment. Interestingly, LAIR-1 deficiency resulted in an increased production of these chemokines. Since previous studies have particularly evidenced that CXCL10 and CCL2 mediate LPS- and influenza-induced ARDS[47–50], this suggests that targeting LAIR-1 in this context can simultaneously affect the secretion of relevant chemokines. Also, an increased number of the heterogeneous CD11b^{high} CD64^{+} population, mainly composed of infiltrating Ly6C^{+} monocytes/macrophages, was observed in the lungs of LAIR-1 KO mice. These results in the ALI/ARDS model are in line with the Keerthivasan et al. study, which shows an increased percentage of Ly6C^{+} infiltrating macrophages in the lungs of LAIR-1 KO mice, while AM were not affected[24]. This leads to the conclusion that LAIR-1 is critically implicated in the dynamic of inflammatory monocyte recruitment to the lungs and differentiation into functional macrophages, shaping the progression and severity of ARDS.

Big data sharing strongly contributes to the advancement of research in the medical field, especially since access to human samples is not an easy option for all research laboratories. In particular, the COVID-19 pandemic was associated with a remarkable reliance on transcriptomic analysis, notably scRNA-seq, that dissects lung immune responses in great detail. Here, we exploited a single-nuclei RNAseq from autopsy lungs and 2 scRNA-seq performed on BAL cells[42,43,45]. Having recently demonstrated that LAIR-1 plays a protective role in allergic asthma, we wanted to assess the regulation of LAIR-1 expression in COVID-19-induced lung injury. Interestingly, data reveal that *LAIR1* is inducible on macrophages from both lungs and BAL of COVID-19 patients. As a matter of fact, *LAIR1* expression correlates with the intensity of inflammatory responses, suggesting LAIR-1 is a potential biomarker of COVID-19 infection and severity. Recent longitudinal single-cell epitope and RNA-sequencing analyses have consistently revealed a negative correlation between IFN-I-stimulated gene and *LAIR1* expression[51]. Since LAIR-1 is identified as an inhibitory receptor equipped with immunoreceptor tyrosine-based inhibitory motifs in the intracellular domain, the induction of this receptor could be explained as a reaction of the immune system to counteract uncontrolled inflammation in the lungs or as an exhaustion phenotype. Similar upregulation was described for other inhibitory receptors such as programmed death-1, T-cell immunoglobulin and mucin domain 3, and TIGIT on T cells from patients with COVID-19[52,53], suggesting a positive correlation between inhibitory checkpoint expression and the severity of COVID-19 infection and/or complications. Therefore, investigating the implication of LAIR-1 with other immune checkpoints could be extremely relevant in the prediction of COVID-19 progression toward fatal ARDS.

The Poly(I:C) mouse model as well as the transcriptomic data from patients with COVID-19 suggest LAIR-1 as a novel actor in lung injury. In particular, our study reveals that LAIR-1 participates in the protection from acute pulmonary inflammation primarily through the regulation of macrophage activation. Therefore, the agonistic activation of LAIR-1 could be a promising therapeutic strategy in acute lung inflammation. As compared to other approaches that neutralize specific inflammatory mediators, such a strategy has the advantage of regulating several inflammatory pathways simultaneously by engaging LAIR-1. Further investigations are thereby required to demonstrate the clinical relevance of these findings and to pave the way for novel targeted therapies in this field.

METHODS

Mice

WT C57BL/6J and LAIR-1 KO mice were purchased from Jackson Laboratory (Bar Harbor, ME, USA). Eight- to twelve-week-old male and female mice were used in the study. The LAIR-1 KO mice have exons 4–8 deleted by homologous recombination. This mutation does not affect the viability, fertility, and lifespan of homozygote mice. All experimentation protocols were approved by the University of Southern California Institutional Animal Care and Use Committee and conducted in accordance with the principles of the Declaration of Helsinki.

ALI model

Mice were sensitized intranasally for 3 days with Poly(I:C) (40 μg per mouse in 40 μL, InvivoGen, San Diego, CA, USA) to induce acute inflammatory lung injury. Control mice received PBS instead of Poly(I:C). To assess lung permeability alterations, mice received FITC-dextran (10 mg/kg, Millipore-Sigma, St. Louis, MO, USA) on day 4 via the intranasal route, 30 minutes before blood collection and euthanasia. FITC fluorescence intensity was measured in the plasma using Synergy 2 microplate reader (BioTek, Winooski, VT, USA). In some experiments, lung function was evaluated on day 4 by direct measurement of lung resistance in restrained, tracheostomized, and mechanically ventilated mice using the FinePointe RC system (Buxco Research Systems, Wilmington, NC, USA) under general anesthesia[54–56]. Mice were sequentially challenged with aerosolized PBS (baseline), followed by increasing doses of methacholine ranging from 5 to 40 mg/mL. Maximum lung resistance values were recorded during a 3-minute period after each methacholine challenge. Data were analyzed by repeated measurements of a general linear model.

Tissue processing and flow cytometry

After euthanasia, lungs were injected with 2 mL of ice-cold PBS to collect BAL cells. The following anti-mouse antibodies were used to identify the main immune populations in the BAL: PE-Cy7 CD45 (clone 30-F11; BioLegend, San Diego, CA, USA), APC-Cy7 CD11c (clone N418; BioLegend), PE Siglec-F (clone E50–2440; BD Pharmagen, Franklin Lakes, NJ, USA), APC Ly6G (clone 1A8; BioLegend), PerCP-Cy5.5 CD3 (clone 17A2; BioLegend), and eFluor450 CD11b (clone M1/70; Invitrogen, Carlsbad, CA, USA). Lung tissue was then cut into small pieces and incubated in type IV collagenase (1.6 mg/mL; Worthington Biochemicals, Lake-wood, NJ, USA) at 37°C for 60 minutes. Single-cell suspensions were obtained by passing the lung tissue digest through a 70 μm cell strainer. Red blood cells were lysed in all cell suspensions using RBC Lysis Buffer from BioLegend. The following antibodies were used for lung immune cell staining: FITC CD45 (30-F11), PerCP-Cy5.5 CD11c (N418), PE-Cy7 Ly6G (1A8), APC or PE CD317 (927), APC-Cy7 Ly6C (HK1.4), BV510 I-A/I-E (M5/114.15.2), APC CD64 (X54–5/7.1) (all from BioLegend) and eFluor450 CD11b (M1/70), and PE LAIR-1 (113) (both from Invitrogen). Neutrophil recruitment to the lungs was considered as a primary outcome measure. All cells were preincubated with anti-mouse CD16/32 (clone 93; BioLegend) to block the Fc receptors. CountBright Absolute Count Beads were used to count lung immune cells (Invitrogen). The acquisition was performed on BD FACSCanto II using the BD FACSDiva

software v8.0.1. Data were analyzed with FlowJo software (TreeStar, Woodburn, OR, USA) version 10.

Macrophage sorting

CD11b^{high} CD64^{+} macrophages were sorted on a FACSARIA III system (Becton Dickinson, Franklin Lakes, NJ, USA) from the lungs of WT and LAIR-1 KO mice after 3 intranasal doses of Poly(I:C). The purity of macrophages was >95% (Supplementary Fig. 1). Cells were directly lysed for RNA extraction or cultured in complete RPMI for cytokine quantification in the supernatant and other functional assays. RNA samples were sequenced on a NextSeq 500 (Illumina, San Diego, CA, USA) system, and analyses were performed using Partek Flow, as previously described[57]. RNA sequencing data are accessible in Genbank via the following code: GSE216259. To assess glucose uptake, sorted macrophages were incubated with 50 μg/mL of 2-(N-[7-nitrobenz-2-oxa-1,3-diazol-4-yl] amino)−2-deoxyglucose for 20 minutes, as previously described[55]. The acquisition was performed using a BD FACSCanto II (BD Biosciences, Franklin Lakes, NJ, USA). To assess phagocytosis, we used the pHrodo Zymosan BioParticles conjugates (ThermoFisher, Waltham, MA, USA)[58]. Sorted macrophages were seeded for 30 min and then incubated for 90 min in the dark, alone or with zymosan bioparticles (5 μg/mL). Phagocytosis was quantified by the increase in particle fluorescence (509/533, FITC/GFP filter) in acidic compartments using flow cytometry.

scRNA-seq analysis

The scRNA-seq data used in this study were acquired from publicly available datasets obtained from 3 different sources: GSE145926, GSE171524, and the dataset from the publication with PMID33765436. All data processing and cell type annotation were performed based on the original publications from each dataset. mRNA expression levels were assessed with normalized values. Prior to analysis, all expression values were normalized using established methods described in the original publications. The inhibitory gene list is a combination of Gene Ontology terms: GO:0002767, GO:0050777, GO:0045824, GO:0002683, GO:0001818, GO:0032682, GO:0050728. Graphs were generated using Partek Flow and R software version 4.3.0. For the scRNA-seq data analysis and visualization, we utilized various R packages, including Seurat (version 4.9.9.9044), ggplot2 (version 3.4.2), and ComplexHeatmap (version 2.16.0).

Protein and cytokine measurement

The BCA Protein Assay was used for colorimetric quantitation of total protein in the BAL (ThermoFisher). The levels of cytokines were measured in the BAL and culture supernatants using Legendplex multiplex kits (BioLegend).

Statistical analysis

The *n* number in mouse lung studies was chosen based on our preliminary data as a reference test to calculate the effect size. Randomization based on a single sequence of random assignments was used to allocate mice to different groups. Treatments and measurements were not performed in an orderly way to minimize confounders. Blinding was

applied, and the genotypes of mice were masked from the Poly(I:C) treatment step until the data had been analyzed. No animals or data points were excluded during the analysis. A 2-tailed Student's *t*-test for unpaired data was applied for comparisons between the 2 groups. Data were analyzed with Prism Software (GraphPad Software Inc, San Diego, CA, USA). Error bars represent the standard error of the mean. A p value < 0.05 was considered to denote statistical significance (*$p < 0.05$, **$p < 0.01$, ***$p < 0.001$, nonsignificant).

Supplementary Material

Refer to Web version on PubMed Central for supplementary material.

ACKNOWLEDGMENTS

The authors are grateful to the USC Libraries Bioinformatics Service for assisting with data analysis, in particular Dr Yibu Chen and Dr Yong-Hwee E Loh. The bioinformatics software and computing resources used in the analysis are funded by the USC Office of Research and the Norris Medical Library

FUNDING

This article was financially supported by National Institutes of Health Public Health Service grants R01 HL144790, R01 HL151493, R01 AI145813, R01 HL151769, and R01 HL159804 (O.A.).

REFERENCES

1. Meyer NJ, Gattinoni L & Calfee CS Acute respiratory distress syndrome. Lancet 398, 622–637 (2021). [PubMed: 34217425]
2. Banavasi H, Nguyen P, Osman H & Soubani AO Management of ARDS - what works and what does not. Am. J. Med. Sci 362, 13–23 (2021). [PubMed: 34090669]
3. Matthay MA et al. Acute respiratory distress syndrome. Natl Rev. Dis. Primer 5, 1–22 (2019).
4. Bellani G et al. Epidemiology, patterns of care, and mortality for patients with acute respiratory distress syndrome in intensive care units in 50 countries. JAMA 315, 788–800 (2016). [PubMed: 26903337]
5. Reiss LK, Schuppert A & Uhlig S Inflammatory processes during acute respiratory distress syndrome: a complex system. Curr. Opin. Crit. Care 24, 1–9 (2018). [PubMed: 29176329]
6. Matuschak GM & Lechner AJ Acute lung injury and the acute respiratory distress syndrome: pathophysiology and treatment. Mo. Med 107, 252–258 (2010). [PubMed: 20806836]
7. Gonzales JN, Lucas R & Verin AD The acute respiratory distress syndrome: mechanisms and perspective therapeutic approaches. Austin J. Vasc. Med 2, 1009 (2015). [PubMed: 26973981]
8. Hasan SS et al. Mortality in COVID-19 patients with acute respiratory distress syndrome and corticosteroids use: a systematic review and meta-analysis. Expert Rev. Respir. Med 14, 1149–1163 (2020). [PubMed: 32734777]
9. Aslan A, Aslan C, Zolbanin NM & Jafari R Acute respiratory distress syndrome in COVID-19: possible mechanisms and therapeutic management. Pneumonia (Nathan) 13, 14 (2021). [PubMed: 34872623]
10. Torres Acosta MA & Singer BD Pathogenesis of COVID-19-induced ARDS: implications for an ageing population. Eur. Respir. J 56, 2002049 (2020).
11. Chimenti L et al. Comparison of direct and indirect models of early induced acute lung injury. Intensive Care Med. Exp 8(Suppl. 1), 62 (2020). [PubMed: 33336290]
12. Matute-Bello G, Frevert CW & Martin TR Animal models of acute lung injury. Am. J. Physiol. Lung Cell. Mol. Physiol 295, L379–L399 (2008). [PubMed: 18621912]
13. Gao X et al. Interleukin-38 ameliorates poly(I:C) induced lung inflammation: therapeutic implications in respiratory viral infections. Cell Death Dis. 12, 53 (2021). [PubMed: 33414457]

14. Huang LY, Stuart C, Takeda K, D'Agnillo F & Golding B Poly(I:C) induces human lung endothelial barrier dysfunction by disrupting tight junction expression of Claudin-5. PLoS One 11, e0160875 (2016). [PubMed: 27504984]
15. Gan T et al. TLR3 regulated poly I:C-induced neutrophil extracellular traps and acute lung injury partly through p38 MAP kinase. Front. Microbiol 9, 3174 (2018). [PubMed: 30622526]
16. Chun CD, Liles WC, Frevert CW, Glenny RW & Altemeier WA Mechanical ventilation modulates Toll-like receptor-3-induced lung inflammation via a MyD88-dependent, TLR4-independent pathway: a controlled animal study. BMC Pulm. Med 10, 57 (2010). [PubMed: 21092115]
17. Chen X et al. Macrophage polarization and its role in the pathogenesis of acute lung injury/acute respiratory distress syndrome. Inflamm. Res 69, 883–895 (2020). [PubMed: 32647933]
18. Tao H, Xu Y & Zhang S The role of macrophages and alveolar epithelial cells in the development of ARDS. Inflammation 46, 47–55 (2023). [PubMed: 36048270]
19. Liu C, Xiao K & Xie L Progress in preclinical studies of macrophage autophagy in the regulation of ALI/ARDS. Front. Immunol 13:922702.
20. Brom VC, Burger C, Wirtz DC & Schildberg FA The role of immune checkpoint molecules on macrophages in cancer, infection, and autoimmune pathologies. Front. Immunol 13:837645. [PubMed: 35418973]
21. Jin J et al. LAIR-1 activation inhibits inflammatory macrophage phenotype in vitro. Cell. Immunol 331, 78–84 (2018). [PubMed: 29887420]
22. Zhang Y et al. The role of LAIR-1 (CD305) in T cells and monocytes/macrophages in patients with rheumatoid arthritis. Cell. Immunol 287, 46–52 (2014). [PubMed: 24380839]
23. Carvalheiro T et al. Leukocyte associated immunoglobulin like Receptor 1 regulation and function on monocytes and dendritic cells during inflammation. Front. Immunol 11, 1793 (2020). [PubMed: 32973751]
24. Keerthivasan S et al. Homeostatic functions of monocytes and interstitial lung macrophages are regulated via collagen domain-binding receptor LAIR1. Immunity 54, 1511–1526.e8 (2021). [PubMed: 34260887]
25. Son M Understanding the contextual functions of C1q and LAIR-1 and their applications. Exp. Mol. Med 54, 567–572 (2022). [PubMed: 35562585]
26. Meyaard L The inhibitory collagen receptor LAIR-1 (CD305). J. Leukoc. Biol 83, 799–803 (2008). [PubMed: 18063695]
27. Meyaard L et al. LAIR-1, a novel inhibitory receptor expressed on human mononuclear leukocytes. Immunity 7, 283–290 (1997). [PubMed: 9285412]
28. Helou DG et al. LAIR-1 acts as an immune checkpoint on activated ILC2s and regulates the induction of airway hyperreactivity. J. Allergy Clin. Immunol 149, 223–236.e6 (2022). [PubMed: 34144112]
29. Verbrugge A, de Ruiter T, Geest C, Coffer PJ & Meyaard L Differential expression of leukocyte-associated Ig-like receptor-1 during neutrophil differentiation and activation. J. Leukoc. Biol 79, 828–836 (2006). [PubMed: 16461736]
30. Son M et al. Evidence for C1q-mediated crosslinking of CD33/LAIR-1 inhibitory immunoreceptors and biological control of CD33/LAIR-1 expression. Sci. Rep 7, 270 (2017). [PubMed: 28325905]
31. Guo N et al. Role and mechanism of LAIR-1 in the development of autoimmune diseases, tumors, and malaria: a review. Curr. Res. Transl. Med 68, 119–124 (2020). [PubMed: 32690423]
32. Kang X et al. The ITIM-containing receptor LAIR1 is essential for acute myeloid leukaemia development. Nat. Cell Biol 17, 665–677 (2015). [PubMed: 25915125]
33. Park JE et al. Leukocyte-associated immunoglobulin-like receptor 1 inhibits T-cell signaling by decreasing protein phosphorylation in the T-cell signaling pathway. J. Biol. Chem 295, 2239–2247 (2020). [PubMed: 31932281]
34. Misharin AV, Morales-Nebreda L, Mutlu GM, Budinger GRS & Perlman H Flow cytometric analysis of macrophages and dendritic cell subsets in the mouse lung. Am. J. Respir. Cell Mol. Biol 49, 503–510 (2013). [PubMed: 23672262]
35. Liu Y et al. LAIR-1 suppresses cell growth of ovarian cancer cell via the PI3KAKT-mTOR pathway. Aging 12, 16142–16154 (2020). [PubMed: 32628130]

36. Hoesel B & Schmid JA The complexity of NF-κB signaling in inflammation and cancer. Mol. Cancer 12, 86 (2013). [PubMed: 23915189]
37. Jin Y et al. Involvement of the PI3K/Akt/NF-κB signaling pathway in the attenuation of severe acute pancreatitis-associated acute lung injury by Sedum sarmentosum Bunge extract. BioMed Res. Int 2017, 9698410 (2017).
38. Willmann EA, Pandurovic V, Jokinen A, Beckley D & Bohlson SS Extracellular signal-regulated kinase 1/2 is required for complement component C1q and fibronectin dependent enhancement of Fcγ- receptor mediated phagocytosis in mouse and human cells. BMC Immunol. 21, 61 (2020). [PubMed: 33317446]
39. Kulkarni HS et al. Update on the features and measurements of experimental acute lung injury in animals: an official American Thoracic Society workshop report. Am. J. Respir. Cell Mol. Biol 66, e1–e14 (2022). [PubMed: 35103557]
40. Gu T et al. Cytokine signature induced by SARS-CoV-2 spike protein in a mouse model. Front. Immunol 11:621441.
41. Bao M, Hofsink N & Plösch T LPS versus Poly I: C model: comparison of long-term effects of bacterial and viral maternal immune activation on the offspring. Am. J. Physiol. Regul. Integr. Comp. Physiol 322, R99–R111 (2022). [PubMed: 34874190]
42. Melms JC et al. A molecular single-cell lung atlas of lethal COVID-19. Nature 595, 114–119 (2021). [PubMed: 33915568]
43. Liao M et al. Single-cell landscape of bronchoalveolar immune cells in patients with COVID-19. Nat. Med 26, 842–844 (2020). [PubMed: 32398875]
44. Rumpret M et al. Functional categories of immune inhibitory receptors. Nat. Rev. Immunol 20, 771–780 (2020). [PubMed: 32612208]
45. Szabo PA et al. Longitudinal profiling of respiratory and systemic immune responses reveals myeloid cell-driven lung inflammation in severe COVID-19. Immunity 54, 797–814.e6 (2021). [PubMed: 33765436]
46. Kumawat K et al. LAIR-1 limits neutrophilic airway inflammation. Front. Immunol 10, 842 (2019). [PubMed: 31080449]
47. Lang S et al. CXCL10/IP-10 neutralization can ameliorate lipopolysaccharide-induced acute respiratory distress syndrome in rats. PLoS One 12, e0169100 (2017). [PubMed: 28046003]
48. Wang W et al. Monoclonal antibody against CXCL-10/IP-10 ameliorates influenza A (H1N1) virus induced acute lung injury. Cell Res. 23, 577–580 (2013). [PubMed: 23419516]
49. Lai C et al. C-C motif chemokine ligand 2 (CCL2) mediates acute lung injury induced by lethal influenza H7N9 virus. Front. Microbiol 8, 587 (2017). [PubMed: 28421067]
50. Williams AE et al. Evidence for chemokine synergy during neutrophil migration in ARDS. Thorax 72, 66–73 (2017). [PubMed: 27496101]
51. van der Wijst MGP et al. Longitudinal single-cell epitope and RNA-sequencing reveals the immunological impact of type 1 interferon autoantibodies in critical COVID-19. bioRxiv 2021.
52. Diao B et al. Reduction and functional exhaustion of T cells in patients with coronavirus disease 2019 (COVID-19). Front. Immunol 11, 827 (2020). [PubMed: 32425950]
53. Bellesi S et al. Increased CD95 (Fas) and PD-1 expression in peripheral blood T lymphocytes in COVID-19 patients (Fas). Br. J. Haematol 191, 207–211 (2020). [PubMed: 32679621]
54. Hurrell BP et al. Cannabinoid receptor 2 engagement promotes group 2 innate lymphoid cell expansion and enhances airway hyperreactivity. J. Allergy Clin. Immunol 149, 1628–1642.e10 (2022). [PubMed: 34673048]
55. Helou DG et al. PD-1 pathway regulates ILC2 metabolism and PD-1 agonist treatment ameliorates airway hyperreactivity. Nat. Commun 11, 3998 (2020). [PubMed: 32778730]
56. Helou DG et al. Human PD-1 agonist treatment alleviates neutrophilic asthma by reprogramming T cells. J. Allergy Clin. Immunol 151, 526–538.e8 (2023). [PubMed: 35963455]
57. Galle-Treger L et al. Autophagy impairment in liver CD11c+ cells promotes non-alcoholic fatty liver disease through production of IL-23. Nat. Commun 13, 1440 (2022). [PubMed: 35301333]
58. Helou DG et al. Nrf2 downregulates zymosan-induced neutrophil activation and modulates migration. PLoS One 14, e0216465 (2019). [PubMed: 31419224]

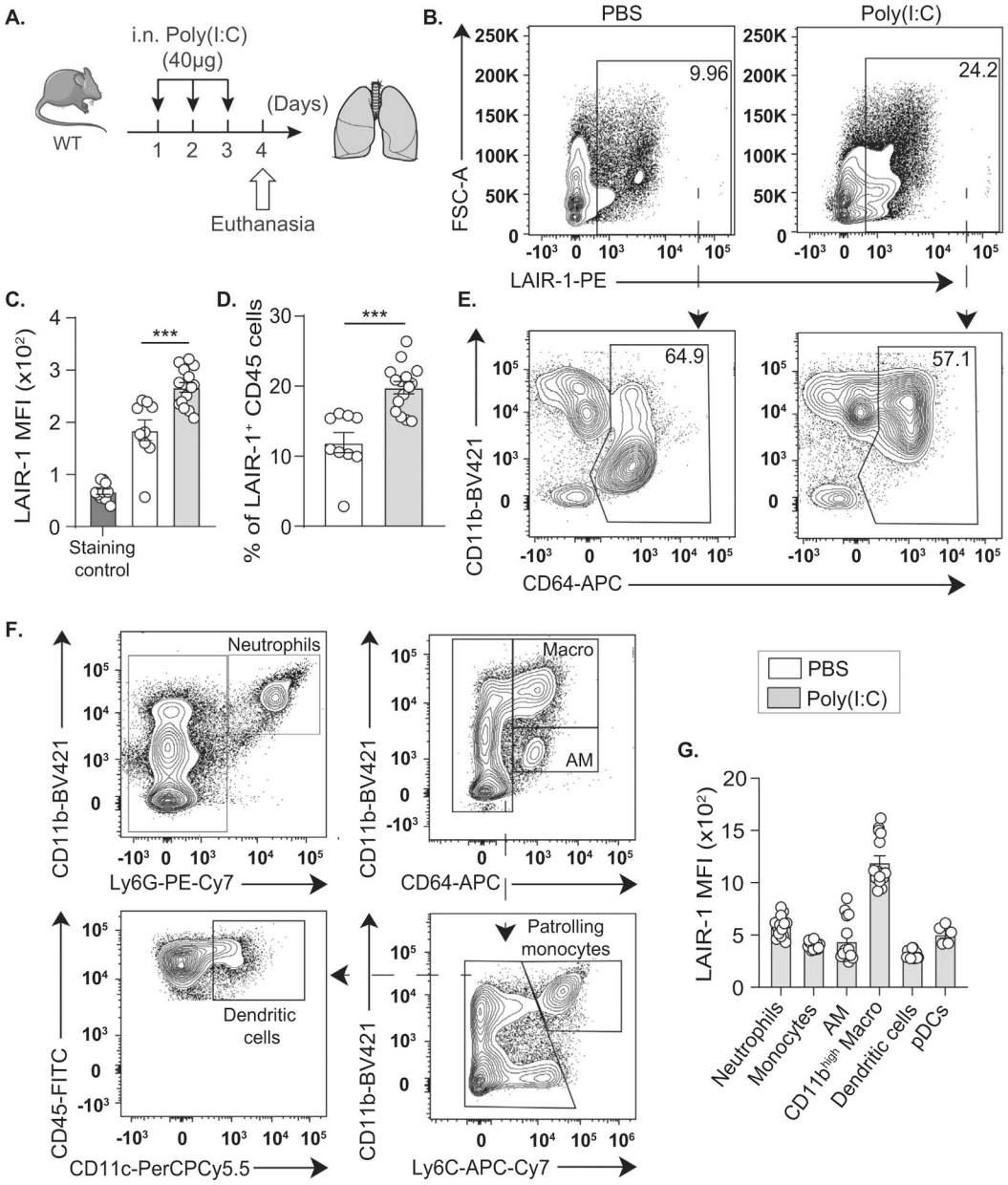

Fig. 1.

LAIR-1 is inducible on pulmonary CD45$^+$ cells in response to Poly(I:C) and is mainly expressed on macrophages. (A) C57BL/6J (WT) mice were intranasally (i.n.) challenged with 40 µg of Poly(I:C) for 3 consecutive days. Control mice received PBS only. On day 4, lungs were collected after euthanasia to perform flow cytometry analysis. (B) Representative flow cytometry plots of LAIR-1 induction on CD45$^+$ cells and corresponding quantifications presented as (C) the mean fluorescence intensity (MFI) of LAIR-1 expression and as (D) the percentage of LAIR-1$^+$ cells in the lungs. (E) Representative flow cytometry plots showing the composition of LAIR-1$^+$ populations in naïve and Poly(I:C)-stimulated mice according to the expression of CD11b and CD64. (F) Flow cytometry plots showing the used gating strategy to identify the main myeloid immune cells in the lungs. (G) The MFI of

LAIR-1 expression on main myeloid pulmonary cells from Poly(I:C)-stimulated mice. Each point on the scatter plots represents data from a single mouse. Data are representative of at least 2 independent experiments and are presented as means ± SEM (2-tailed Student's *t*-test). Images are provided with permission from Servier Medical Art. LAIR-1, leukocyte-associated immunoglobulin-like receptor-1; PBS, phosphate buffer saline; WT, wild-type

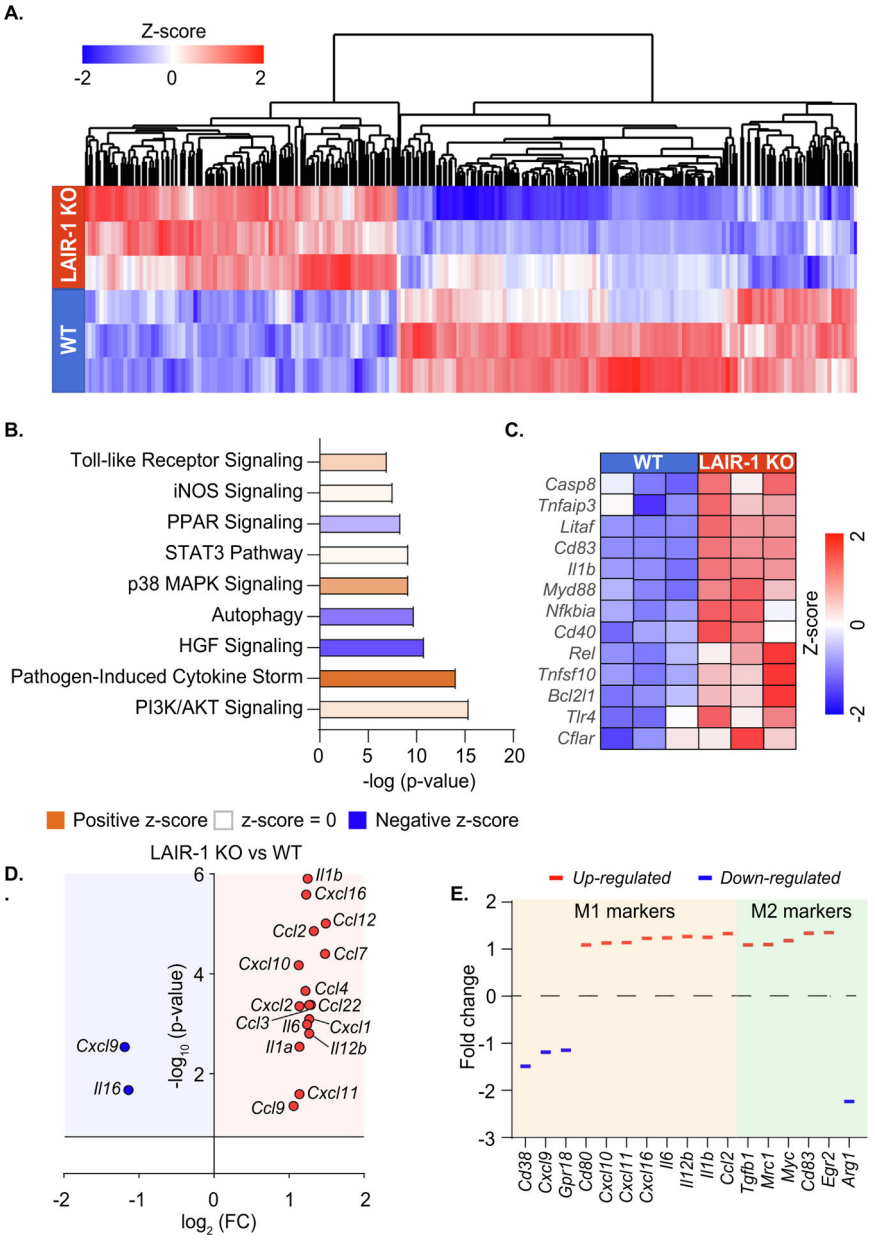

Fig. 2.

LAIR-1 deficiency potentiates the expression of main inflammatory pathways in lung macrophages. WT and LAIR-1 KO mice were intranasally challenged with 40 μg of Poly(I:C) for 3 consecutive days. On day 4, lungs were collected after euthanasia, and CD11b^{high} CD64^{+} macrophages were FACS-sorted to perform RNAseq analysis. (A) Heatmap representation of total differentially regulated genes, generated with a gene-specific analysis algorithm (counts <20, $p < 0.05$; $n = 3$). (B) Pathway analysis enriched for relevant upregulated genes in LAIR-1 KO macrophages. (C) Heatmap representation of differentially regulated genes involved in NF-κB signaling pathway. (D) Focused volcano plot representing significantly regulated cytokines in LAIR-1 KO macrophages as compared with WT macrophages. (E) The regulation of genes encoding for relevant M1/M2

markers represented as fold changes (LAIR-1 KO/WT). FACS, fluorescence-activated cell sorting; KO, knockout; LAIR-1, leukocyte-associated immunoglobulin-like receptor-1; NF-kB, nuclear factor-κB; RNAseq, RNA sequencing; WT, wild-type.

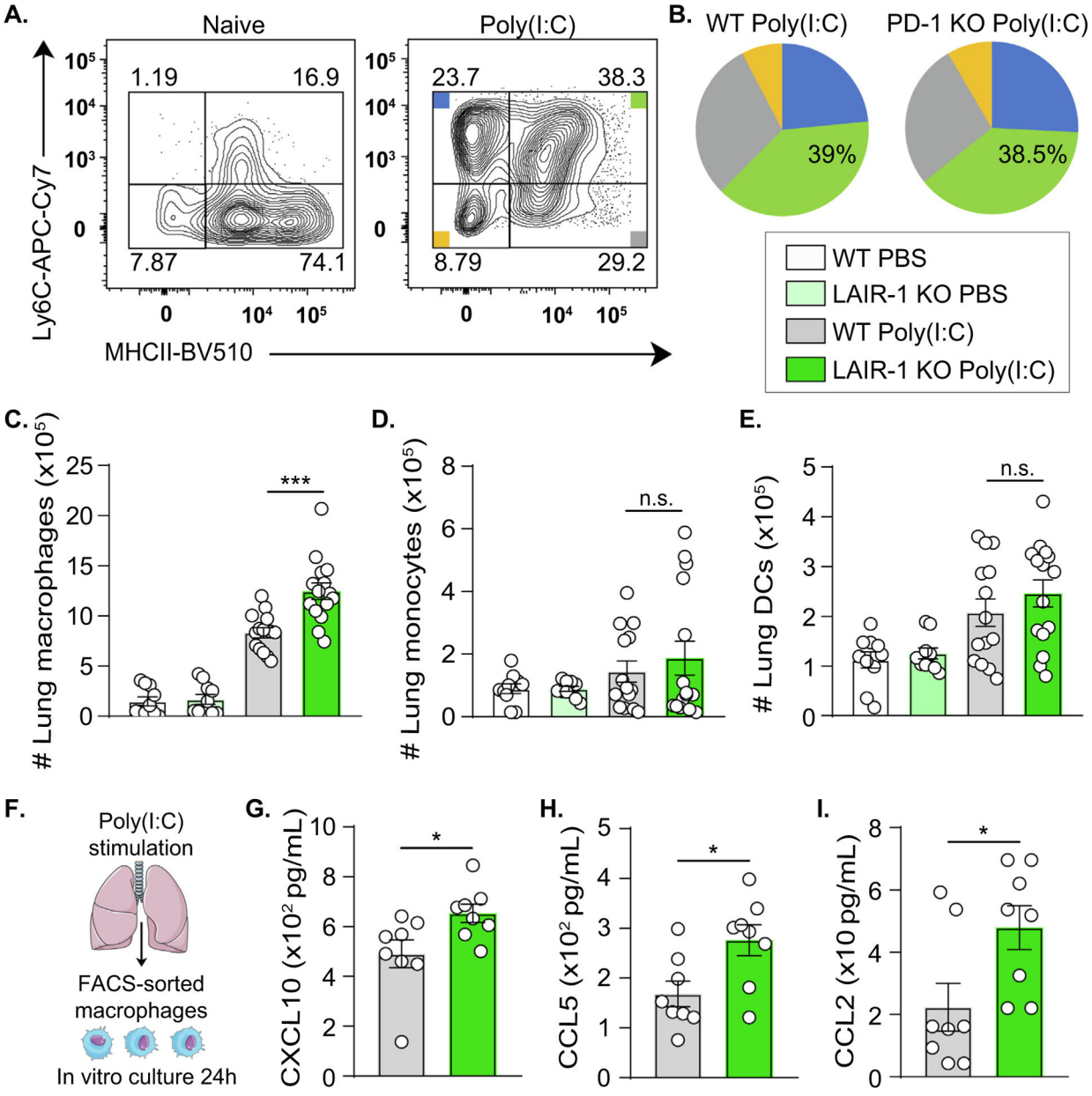

Fig. 3.

LAIR-1 deficiency increases macrophage recruitment and chemokine production. WT and LAIR-1 KO mice were intranasally challenged with 40 μg of Poly(I:C) for 3 consecutive days. On day 4, lungs were collected after euthanasia to perform flow cytometry analysis. (A) The distribution of the different subsets of CD11b^{high} CD64^{+} macrophages according to MHCII and Ly6C expression, represented in flow cytometry plots and as (B) the averages of subset percentages. (C) Total number of CD11b^{high} CD64^{+} macrophages, (D) patrolling monocytes, and (E) DCs in the lungs. (F) After 3 days of Poly(I:C) challenges, lungs were collected, and CD11b^{high} CD64^{+} macrophages were FACS sorted to be cultured *in vitro* for 24 hours. (G) Levels of CXCL-10, (H) CCL5, and (I) CCL2 were quantified in supernatants of macrophage culture. Each point on the scatter plots represents data from a single mouse.

Data are representative of at least 2 independent experiments and are presented as means ± SEM (2-tailed Student's *t*-test). Images are provided with permission from Servier Medical Art. FACS, fluorescence-activated cell sorting; KO, knockout; LAIR-1, leukocyte-associated immunoglobulin-like receptor-1; Poly(I:C), polyinosinic:polycytidylic acid; WT, wild-type.

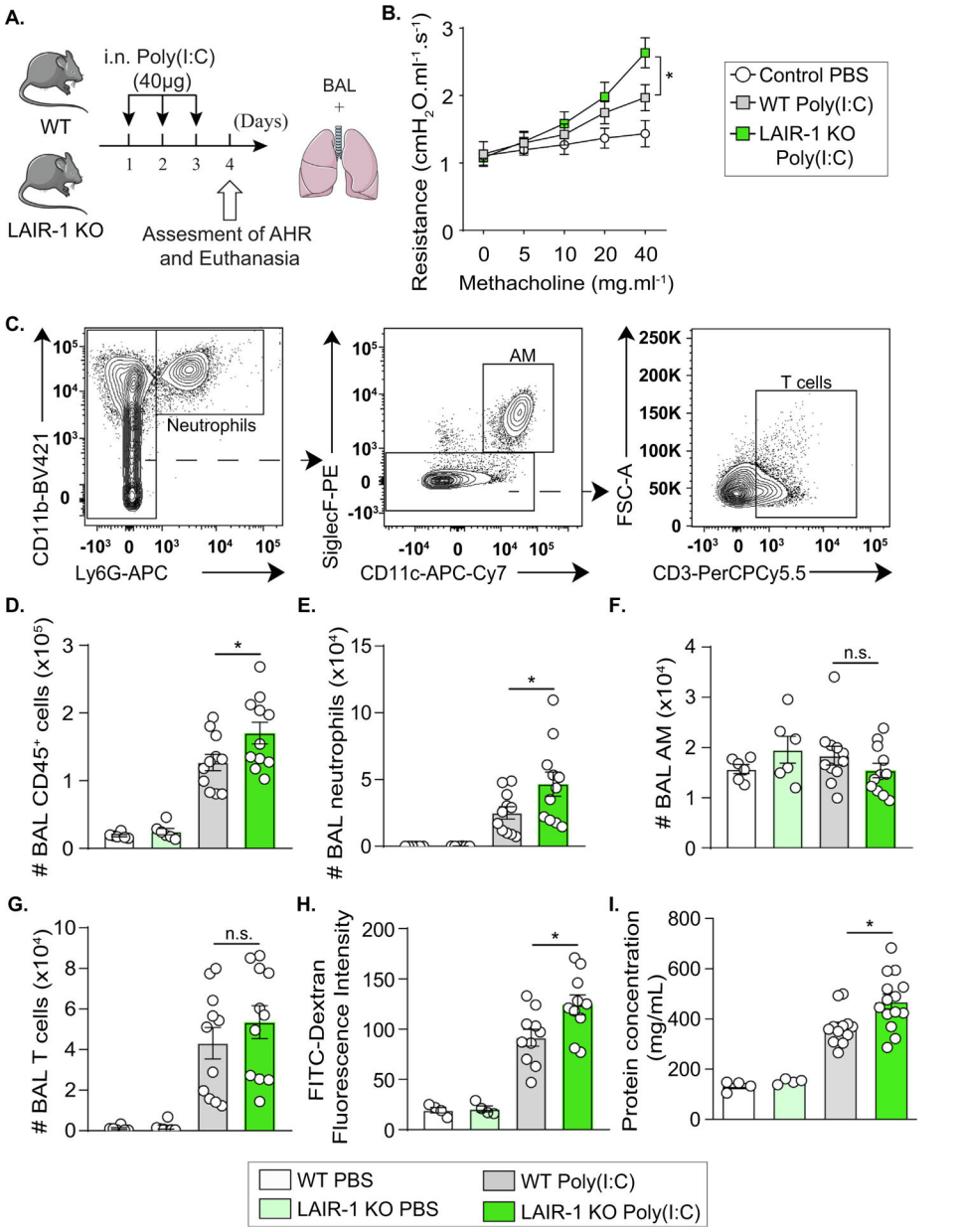

Fig. 4.

LAIR-1 deficiency increases lung resistance, inflammation, and permeability. (A) WT and LAIR-1 KO mice were intranasally challenged with 40 µg of Poly(I:C) for 3 consecutive days. On day 4, lung function was measured, and the BAL was collected. (B) Lung resistance measured in tracheostomized ventilated mice. (C) The gating strategy of neutrophils, AM, and T cells in the BAL. (D) Absolute count of $CD45^+$ cells, (E) neutrophils, (F) AM, and (G) T cells quantified in the BAL. (H) FITC-Dextran fluorescence intensity in the plasma. (I) Total protein concentration in the BAL assessed by the BCA method. Each point on the scatter plots represents data from a single mouse. Data are representative of at least 2 independent experiments and are presented as means ± SEM (2-tailed Student's *t*-test). Images are provided with permission from Servier Medical

Art. AM, alveolar macrophage; BAL, bronchoalveolar lavage; KO, knockout; LAIR-1, leukocyte-associated immunoglobulin-like receptor-1; Poly(I:C), polyinosinic:polycytidylic acid; WT, wild-type.

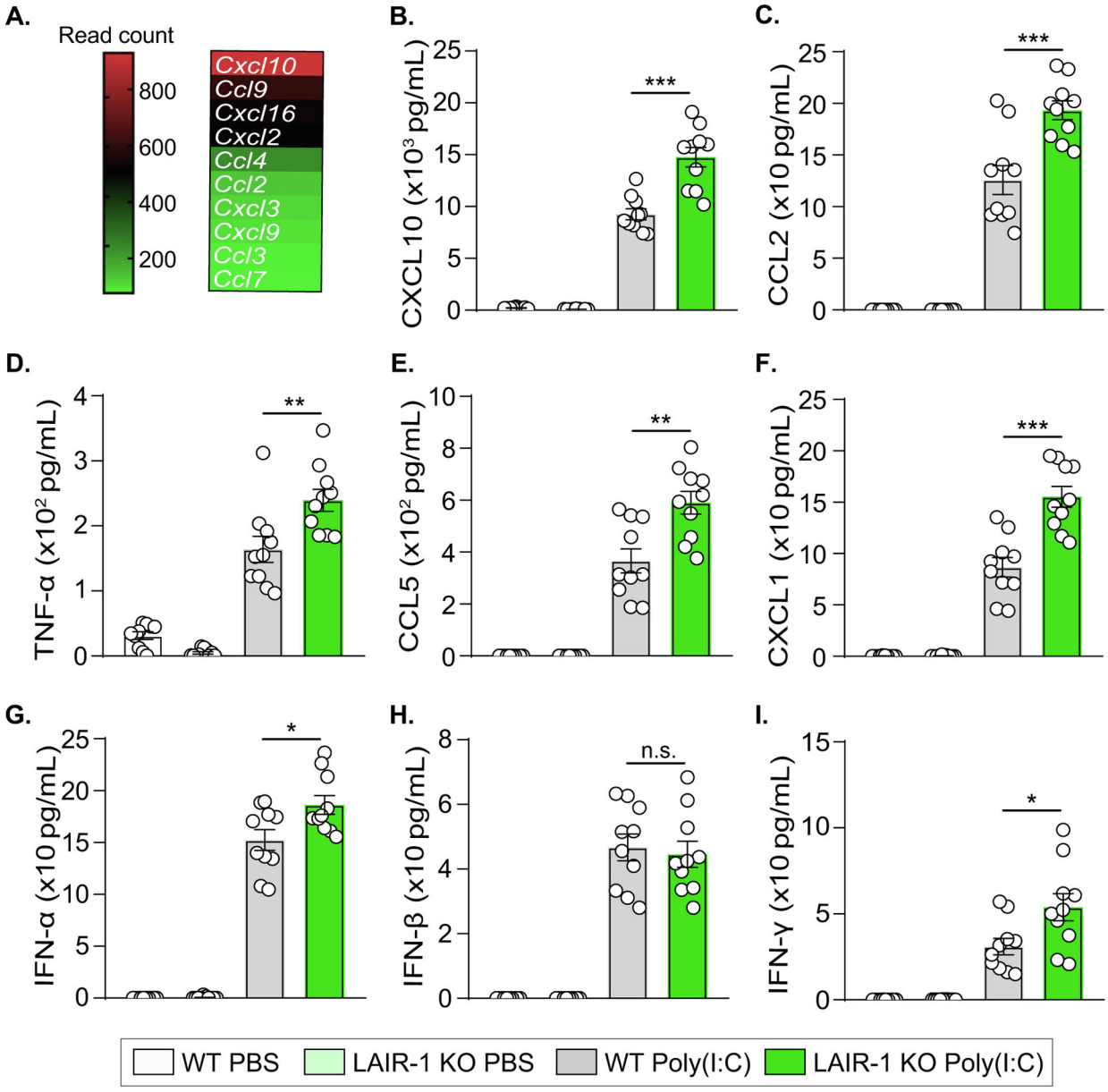

Fig. 5.

LAIR-1 reduces the production of key chemokines in acute lung inflammation. WT and LAIR-1 KO mice were intranasally challenged with 40 μg of Poly(I:C) for 3 consecutive days. On day 4, BAL was collected to measure different cytokine levels. (A) Heatmap representation of the top expressed chemokine genes in macrophages from the lungs of Poly(I:C)-stimulated mice. (B) Levels of CXCL10, (C) CCL2, (D) TNF-α, (E) CCL5, (F) CXCL1, (G) IFN-α, (H) IFN-β, and (I) IFN-γ quantified in the BAL. Each point on the scatter plots represents data from a single mouse. Data are representative of at least 2 independent experiments and are presented as means ± SEM (2-tailed Student's *t*-test). BAL, bronchoalveolar lavage; IFN, interferon; KO, knockout; LAIR-1, leukocyte-associated immunoglobulin-like receptor-1; Poly(I:C), polyinosinic: polycytidylic acid; TNF-α, tumor necrosis factor-alpha; WT, wild-type.

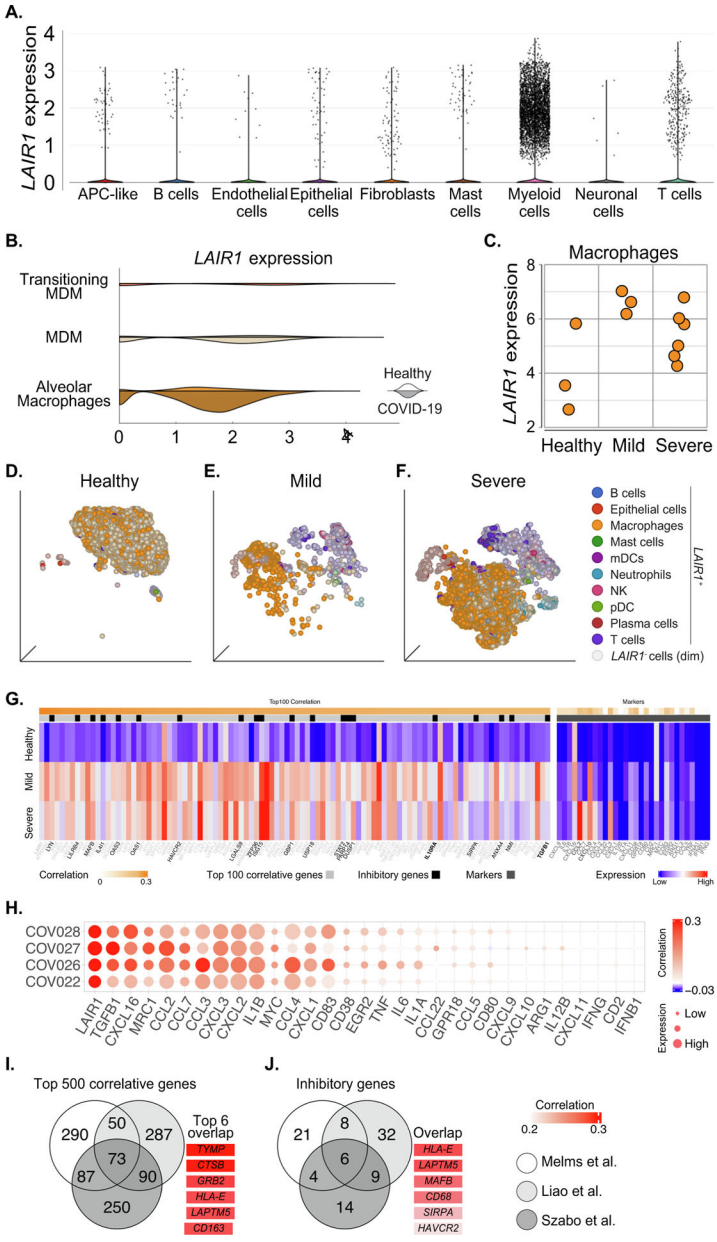

Fig. 6.

LAIR-1 expression is upregulated on macrophages from patient lungs with COVID-19. (A, B) Single-nuclei RNAseq data from a human cohort comprising 19 COVID-19 autopsy lungs and 7 healthy controls with short postmortem interval autopsies. (A) UMAP clustering showing the expression of *LAIR1* in main lung cell populations. (B) Comparison of *LAIR1* expression between myeloid cell populations from COVID-19 patients and healthy controls. (C) LAIR-1 expression in lung macrophages from healthy controls and patients with varying severity of COVID-19. (D) tSNE plots (2D graph) showing $LAIR1^{+}$ and $LAIR1^{-}$ cells (bright *vs.* dim colored, normalized *LAIR1* > 0) in the BAL of healthy donors, (E) mild and (F) severe patients with COVID-19. (G) Heatmap representing the Pearson correlation between *LAIR1* expression and a list of genes in BAL macrophages from healthy

donors, mild and severe patients with COVID-19. (H) A bubble heatmap showing the Pearson correlation between *LAIR1* expression and a list of genes in BAL macrophages from 4 severe patients with COVID-19. (I) Venn diagrams showing overlaps among the top 500 correlative genes from 3 different studies and (J) among a list of inhibitory genes. Graph A is provided with permission from https://singlecell.broadinstitute.org. BAL, bronchoalveolar lavage; COVID-19, coronavirus disease 2019; LAIR-1, leukocyte-associated immunoglobulin-like receptor-1; RNAseq, RNA sequencing; UMAP, Uniform manifold approximation and projection.